

## 2010年度 環境物質工学科 研究報告

1. ポリ乳酸系ナノ粒子の調製と光線力学的治療への応用, 小野努, 大河原賢一, ケミカルエンジニアリング, Vol. 55, pp.63-69, 2010
2. ホウケイ酸ガラスの構造と塩基度, 難波徳郎, 崎田真一, 紅野安彦, 三浦嘉也, *NEW GLASS*, Vol. 25, No. 4, pp. 28-32, 2010
3. *Poly[2,6-(1,4-phenylene)-benzobisimidazole] Nanofiber Networks*, Jin Gong, Testuya Uchida, Shinichi Yamazaki, Kunio Kimura, *Macromolecular Chemistry and Physics* Vol. 211, No. 20, pp. 2226-2232, 2010
4. *Poly(2,5-benzimidazole) nanofibers prepared by reaction-induced crystallization*, Kazuya Kimura, Gong Jin, Shin-ichiro Kohama, Shinichi Yamazaki, Testuya Uchida, Kunio Kimura, *Polymer Journal*, Vol. 42, No. 5, pp. 375-382, 2010
5. *Thermally Induced Solid-State Synthesis of Fluorine-Containing Poly(ether oxadiazole)*, Yuka Maruyama, Yukihiro Maeda, Kanji Wakabayashi, Shinichi Yamazaki, Kunio Kimura, *Journal of Applied Polymer Science*, Vol. 118, No. 1, pp. 91-98, 2010
6. *Gasification of woody biomass char with CO<sub>2</sub>: The catalytic effects of K and Ca species on char gasification reactivity*, Keiichirou MITSUOKA, Shigeya HAYASHI, Hiroshi AMANO, Kenji KAYAHARA, Eiji SASAOKA, UDDIN Md. Azhar, *Fuel Processing Technology*, Vol. 92, pp. 26-31, 2010
7. *Study of the Mercury Sorption Mechanism on Activated Carbon in Coal Combustion Flue Gas by the Temperature-Programmed Decomposition Desorption Technique*, Atsushi MURAKAMI, UDDIN Md. Azhar, Ryota OCHIAI, Eiji SASAOKA, Shengji WU, *Energy & Fuels*, Vol. 24, No. 8, pp 4241-4249, 2010
8. *PEG-PLA nanoparticles prepared by emulsion solvent diffusion using oil-soluble and water-soluble PEG-PLA*, Makoto Muranaka, Ken Hirota, Tsutomu Ono, *Mater. Lett.*, vol. 64, pp. 969-971, 2010
9. *Photocatalytic water treatment over WO<sub>3</sub> under visible light irradiation combined with ozonation*, Shunsuke Nishimoto, Takayuki Mano, Yoshikazu Kameshima, Michihiro Miyake, *Chem. Phys. Lett.*, Vol. 500, pp. 86-89, 2010
10. *Steam reforming of naphthalene as model biomass tar over iron-aluminum and Iron-zirconium oxide catalysts*, Hiroyuki NOICHI, UDDIN Md. Azhar, Eiji SASAOKA, *Fuel Processing Technology*, Vol. 91, pp.1609-1616, 2010
11. *Phase separation of borosilicate glass containing sulfur*, Keiji SAIKI, Shinichi SAKIDA, Yasuhiko BENINO, Tokuro NANBA, *J. Ceram Soc. Jpn*, Vol. 118, No. 7, pp. 603-607, 2010
12. *Electrode properties of the Ruddlesden-Popper series,  $\text{La}_{n+1}\text{Ni}_n\text{O}_{3n+1}$  ( $n = 1, 2$  and  $3$ ), as intermediate-temperature solid oxide fuel cells*, Suguru Takahashi, Shunsuke Nishimoto, Motohide Matsuda, Michihiro Miyake, *J. Am. Ceram. Soc.*, Vol. 93, pp. 2329-2333, 2010
13. *A versatile biodegradable polymer with a thermo-reversible/irreversible transition*, Fumiaki Tanimoto, Yoshiro Kitamura, Tsutomu Ono, Hidekazu Yoshizawa, *ACS Appl. Mater. Interfaces*, vol. 2, pp. 606-610, 2010

## ポリ乳酸系ナノ粒子の調製と光線力学的治療への応用

*Preparation of polyoxyethylene-polylactide (PEG-PLA) Nanoparticles and the application in photodynamic therapy (PDT)*

小野 努<sup>\*1)</sup>, 大河原賢一<sup>2)</sup>  
ONO Tsutomu<sup>\*1)</sup>, OGAWARA Ken-ichi<sup>2)</sup>

### ■ 概 要 ■

光線力学的治療（PDT）は、光増感剤を体内に投与後、外部から腫瘍近傍にのみ光照射することで局所的な抗がん治療を実現する低侵襲性治療法であり、国内でも 1994 年に厚生労働省の認可を受け早期がんに対する治療が行われている。しかしながら、腫瘍近傍への光増感剤の選択的送達は十分でなく光過敏症といった副作用が生じる。本研究では、生体適合性および生分解性を有するポリ乳酸系ナノ粒子へ高効率で光増感剤を内封する技術を確認し、血中滞留性に優れた薬物キャリアを開発して、その PDT における治療効果を生体外および生体内で検証した。その結果、非常に高い血中滞留性と Enhancement of permeability and retention (EPR)効果による腫瘍近傍への確実な集積が確認され、PDT による腫瘍の増殖抑制効果が示された。本論文では、PDT の現状から光増感剤内封ナノ粒子を用いた PDT の有効性について分かりやすく解説した。

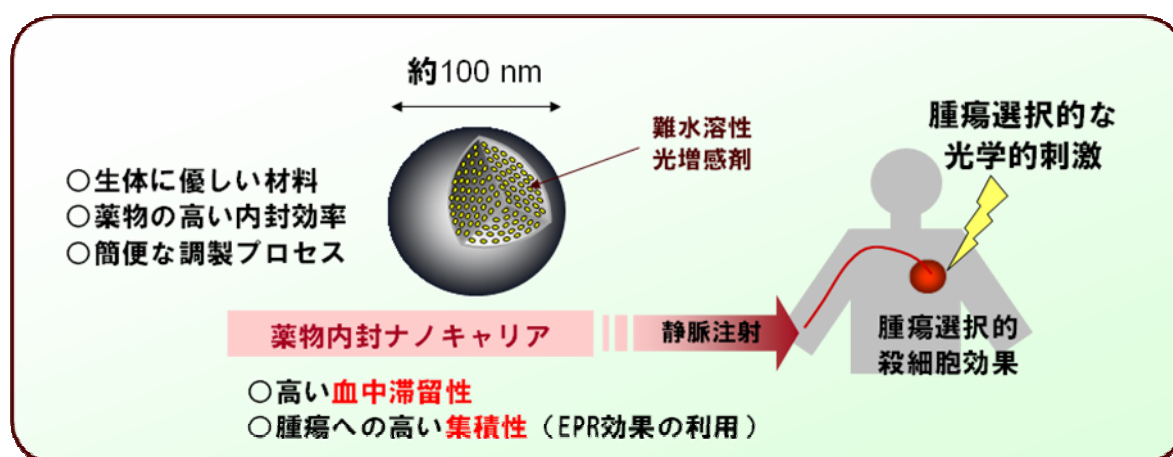


図 薬物内封ナノ粒子を利用した光線力学的治療の概念図

### ■ キーワード ■

光線力学的治療, 光増感剤, ドラッグデリバリー, ナノ粒子

### ■ 所 属 ■

- 1) 環境物質工学科 准教授
- 2) 医歯薬総合研究科 准教授

### ■ 掲載先 ■

ケミカルエンジニアリング, Vol.55, pp.63-69 (2010)

# ホウケイ酸ガラスの構造と塩基度

## Structure and Basicity of Borosilicate Glasses

難波徳郎<sup>1)</sup>, 崎田真一<sup>2)</sup>, 紅野安彦<sup>3)</sup>, 三浦嘉也<sup>4)</sup>

NANBA Tokuro<sup>1)</sup>, SAKIDA Shinichi<sup>2)</sup>, BENINO Yasuhiko<sup>3)</sup>, MIURA Yoshinari<sup>4)</sup>

### ■ 概 要 ■

材料の物性は構造（原子配列，電子状態）に支配される。構造が塩基度の影響を受けるのであれば，塩基度はガラスの物性と構造の両者の支配因子であり，組成－構造－物性の相関を網羅的に記述することが可能な概念と言える。組成設計で新たな成分の添加を検討することもあると思うが，添加によって物性がどのように変化するか予測するのは困難である。塩基度に基づいてガラスの構造や物性を予測することが可能になれば，材料開発における新たな指針を得ることができる。本稿ではホウケイ酸塩ガラスを例に，塩基度とガラス構造の関係について研究結果を紹介した。

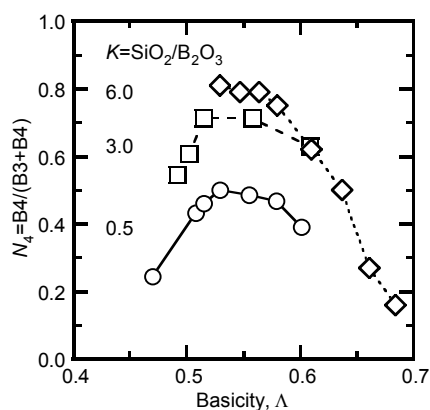


図1  $^{11}\text{B}$  MAS-NMR 測定により求めた  $R \text{Na}_2\text{O} \cdot \text{B}_2\text{O}_3 \cdot K \text{SiO}_2$  ガラス中の 4 配位ホウ素の分率  $N_4$  の塩基度依存性

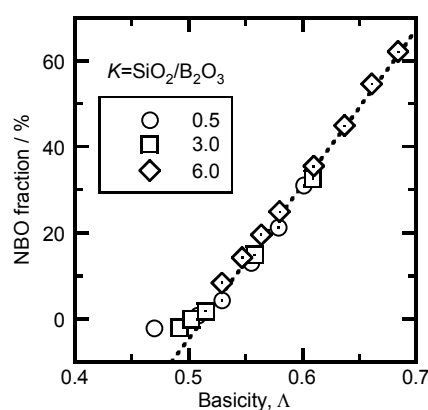


図2  $^{11}\text{B}$  MAS-NMR 測定により求めた  $R \text{Na}_2\text{O} \cdot \text{B}_2\text{O}_3 \cdot K \text{SiO}_2$  ガラス中の非架橋酸素の分率の塩基度依存性

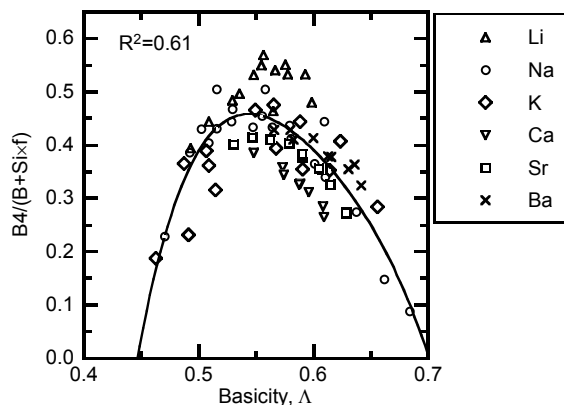


図3 3 成分系ホウケイ酸塩ガラス中の 4 配位ホウ素の分率， $\text{B}_4/(\text{B}+\text{Si} \times f)$  と塩基度の関係

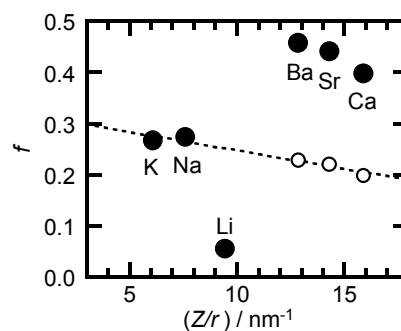


図4 3 成分系ホウケイ酸塩ガラスの係数  $f$  と場の強さ  $Z/r$  の関係（○はアルカリ土類の係数  $f$  を半分にしたもの）

### ■ キーワード ■

ガラス構造，ホウケイ酸塩ガラス，塩基度，構造予測

### ■ 所 属 ■

1) 環境物質工学科 教授，2) 環境管理センター 助教，  
3) 環境物質工学科 准教授，4) 環境物質工学科 名誉教授

### ■ 掲載先 ■

NEW GLASS, Vol. 25(4), pp. 28-32, 2010.12.

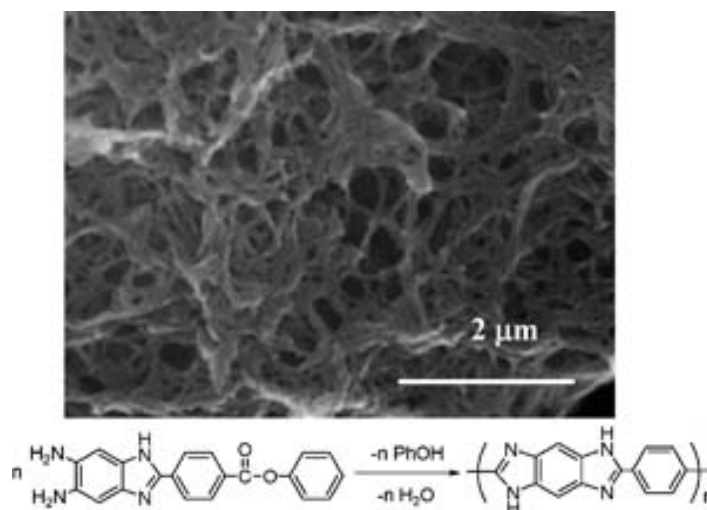
査読：なし，言語：日本語

## Poly[2,6-(1,4-phenylene)-benzobisimidazole] Nanofiber Networks

Jin Gong<sup>1)</sup>, Testuya Uchida<sup>2)</sup>, Shinichi Yamazaki<sup>3)</sup>, Kunio Kimura<sup>4)</sup>

### ■ Summary ■

The preparation of poly[2,6-(1,4-phenylene)-benzobisimidazole] (PPBI) nanofibers was examined using the crystallization of oligomers during isothermal polymerization of self-polymerizable 2-(1,4-carbophenoxyphenyl)-5,6-diaminobenzimidazole. The polymerization was carried out at 350 degrees C at a concentration of 1w.t.-% for 6 h in three kinds of solvent. The solvent influenced the morphology of PPBI precipitates significantly, and PPBI nanofiber networks were successfully formed in DBT, of which the width ranged from 30 to 110 nm. Molecules were aligned along the long axis of nanofibers. A fibrillar morphology with molecular orientation is ideal for high performance materials such as reinforcements, non-woven fabrics and so on. The nanofiber networks exhibit the highest thermal stability.



### ■ Key word ■

Fibers, Heteroatom-containing polymers, High performance polymers, Morphology, Phase separation

### ■ Affiliation ■

- 1) Postdoctoral fellow, Graduate School of Environmental Science
- 2) Master candidate, Graduate School of Natural Science and Technology
- 3) Associate Professor, Dept. of Environmental Chemistry and Materials
- 4) Professor, Dept. of Environmental Chemistry and Materials

### ■ Printing ■

Macromolecular Chemistry and Physics Vol. 211, No. 20, pp. 2226-2232, 2010. DOI: 10.1002/macp.201000306

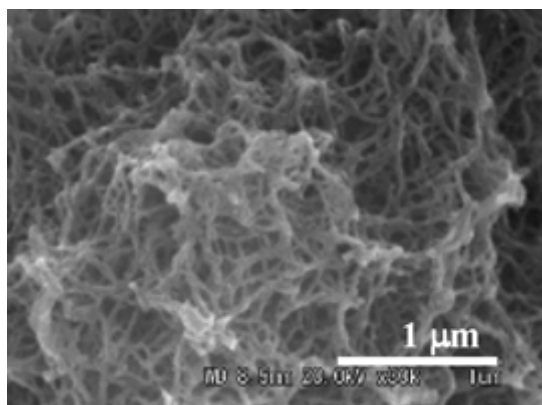
Refreeing: Full paper, Language: English

## ***Poly(2,5-benzimidazole) nanofibers prepared by reaction-induced crystallization***

Kazuya Kimura<sup>1)</sup>, Gong Jin<sup>2)</sup>, Shin-ichiro Kohama<sup>2)</sup>, Shinichi Yamazaki<sup>3)</sup>, Testuya Uchida<sup>4)</sup>, Kunio Kimura<sup>5)</sup>

### ■ Summary ■

Morphological control of poly(2,5-benzimidazole) (PBI) was examined by reaction-induced phase separation of oligomers during polymerization to prepare nanofibers. Three monomers, 3,4-diaminobenzoic acid (DABA), 3,4-diacetoamidebenzoic acid (DAcBA) and phenyl 3,4-diaminobenzoate (PDAB), were used to synthesize PBI. Polymerizations were carried out at 350 °C in a mixture of dibenzyltoluene isomers. Polymerization of DABA yielded spheres with plate-like crystals on their surface. Polymerization of DAcBA yielded almost no precipitates because of the high solubility of DAcBA oligomers. By contrast, polymerization of PDAB yielded aggregates of PBI nanofibers (of which the average diameter was similar to 60 nm), which resembled nonwoven fabrics. These fibers were formed by precipitation of (2,5-benzimidazole) oligomers and their subsequent polymerization into a developing crystal structure. The structure of the monomer significantly influenced the morphology of the PBI product, and PDAB was preferable for the preparation of PBI nanofibers. The temperature of 10% N<sub>2</sub> weight loss in these nanofibers was in the range of 634-644 °C and they were thermally stable.



The network aggregates of poly(2,5-benzimidazole) nanofibers were prepared by the polymerization of phenyl 3,4-diaminobenzoate at 350 °C in a mixture of dibenzyltoluene isomers. The average diameter of the fibers was ~60 nm. These fibers were formed by the crystallization of oligoimidazoles and the subsequent polymerization in them.

### ■ Key word ■

Heterocyclic polymer, Nanofiber, Phase separation, Polybenzimidazole

### ■ Affiliation ■

- 1) Master candidate, Graduate School of Environmental Science
- 2) Postdoctoral fellow, Graduate School of Environmental Science
- 3) Associate Professor, Dept. of Environmental Chemistry and Materials
- 4) Master candidate, Graduate School of Natural Science and Technology
- 5) Professor, Dept. of Environmental Chemistry and Materials

### ■ Printing ■

*Polymer Journal*, Vol. 42, No. 5, pp. 375-382, 2010. DOI: 10.1038/pj.2010.20

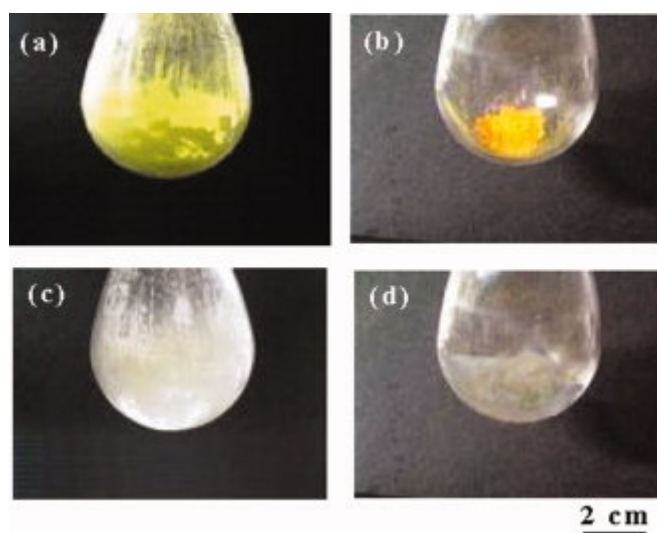
Refreeing: Full paper, Language: English

## Thermally Induced Solid-State Synthesis of Fluorine-Containing Poly(ether oxadiazole)

Yuka Maruyama<sup>1)</sup>, Yukihiro Maeda<sup>1)</sup>, Kanji Wakabayashi<sup>2)</sup>, Shinichi Yamazaki<sup>3)</sup>, Kunio Kimura<sup>4)</sup>

### ■ Summary ■

Synthesis of poly[oxy-(2,3,5,6-tetrafluoro-1,4-phenylene)-(1,3,4-oxadiazol-2-yl)-1,4-phenylene] (F-PEOz) was examined by nucleophilic aromatic substitution reaction of 2-(4-hydroxyphenyl)-5-pentafluorophenyl-1,3,4-oxadiazole (HPOz). Only low molecular weight F-PEOz or crosslinked insoluble polymers were obtained by the solution polymerization with bases. In contrast, thermally induced solid-state polymerization of HPOz potassium salts at 180 °C for 1 h gave fully soluble F-PEOz with the yield of 84% and its reduced viscosity was 0.66 dL g<sup>-1</sup>. The longer polymerization time gave insoluble polymers due to the crosslinking reaction even in solid state. The solid-state polymerization did not undergo topochemically and it proceeded in an amorphous state. The crosslinking reaction was slightly inhibited by the solid-state polymerization. F-PEOz exhibited excellent solubility, high T<sub>g</sub> of 246 °C and good thermal stability.



Polymerization features in solid state during polymerization at 180°C for (a) 0 min (HPOzK), (b) 0.5 min, (c) 5 min, and (d) 1 h.

### ■ Key word ■

High-performance polymer, Heteroatom-containing polymer, Fluorine-containing polymer, Poly(ether oxadiazole), Solid-state polymerization

### ■ Affiliation ■

- 1) Master candidate, Graduate School of Environmental Science
- 2) Postdoctoral fellow, Graduate School of Environmental Science
- 3) Associate Professor, Dept. of Environmental Chemistry and Materials
- 4) Professor, Dept. of Environmental Chemistry and Materials

### ■ Printing ■

Journal of Applied Polymer Science, Vol. 118, No. 1, pp. 91-98, 2010. DOI: 10.1002/app.32391

Refreeing: Full paper, Language: English

## ***Gasification of woody biomass char with CO<sub>2</sub>: The catalytic effects of K and Ca species on char gasification reactivity***

MITSUOKA Keiichirou<sup>1)</sup>, HAYASHI Shigeya<sup>2)</sup>, AMANO Hiroshi<sup>3)</sup>, KAYAHARA Kenji<sup>4)</sup>, SASAOKA Eiji<sup>5)</sup>, UDDIN Md. Azhar<sup>6)</sup>

### ■ Summary ■

The effects of alkali and alkaline earth metals such as potassium (K) and calcium (Ca) on CO<sub>2</sub> gasification reactivity of Japanese cypress (hinoki) char under various temperatures (1123–1223 K) and CO<sub>2</sub> concentration (20–80 vol.%) were studied using thermal gravimetric analysis. The presence of K and Ca compounds in char improved the reactivity of hinoki char for CO<sub>2</sub> gasification catalytically. It was also confirmed that K and Ca compounds can be supported on char to exhibit an enhanced catalytic effect during CO<sub>2</sub> gasification of K-char and Ca-char. The char gasification rate increased with the increase of CO<sub>2</sub> concentration at higher temperatures (1173–1223 K), however at lower temperature (1123 K) the gasification rate decreased at 80% CO<sub>2</sub>. The retardation of char gasification rate at higher CO<sub>2</sub> concentration is caused by the inhibition effect of CO: CO is disproportionated on alkali metal catalysts to CO<sub>2</sub> and carbon, and affected the CO<sub>2</sub> gasification rate. The dependence of char gasification rate on reaction temperature indicated that there was no significant change in the gasification mechanism in the temperature range of 1123–1223 K.

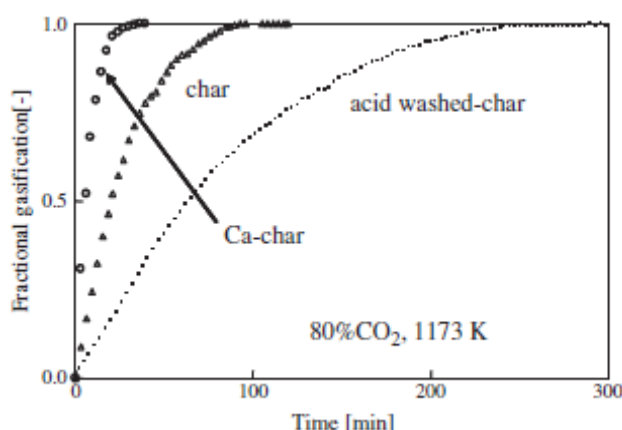


Fig. Fractional gasification of char, Ca-char and acid washed char with CO<sub>2</sub>.

### ■ Key word ■

Biomass char, CO<sub>2</sub> gasification, Alkali and alkaline earth metals

### ■ Affiliation ■

- 1) Master candidate, Graduate School of Environmental Science
- 2) Staff of Ube Industries, Ltd.,
- 3) Staff Ube Industries, Ltd.
- 4) Master candidate, Graduate School of Environmental Science
- 5) Professor Emeritus, Dept. of Environmental Chemistry and Materials
- 6) Associate Professor, Dept. of Environmental Chemistry and Materials

### ■ Printing ■

Fuel Processing Technology, 92, pp. 26–31, 2010.

Refereeing: Full paper, Language: English

# Study of the Mercury Sorption Mechanism on Activated Carbon in Coal Combustion Flue Gas by the Temperature-Programmed Decomposition Desorption Technique

MURAKAMI Atsushi<sup>1)</sup>, UDDIN Md. Azhar<sup>2)</sup>, OCHIAI Ryota<sup>3)</sup>, SASAOKA Eiji<sup>4)</sup> and WU Shengji<sup>5)</sup>

## ■ Summary ■

Effects of coexistent gases (HCl, SO<sub>2</sub>, O<sub>2</sub>, CO<sub>2</sub>, and H<sub>2</sub>O) in simulated coal combustion flue gas on mercury removal by a commercial activated carbon (coconut shell AC) were investigated in a laboratory-scale fixed-bed reactor at 80 °C. To clarify the contribution of the Deacon reaction  $2\text{HCl} + 1/2\text{O}_2 = \text{Cl}_2 + \text{H}_2\text{O}$  (1) on the mercury sorption mechanisms, the experiments were also conducted in the presence of Cl<sub>2</sub> (in the absence of HCl). It was found that O<sub>2</sub> promoted mercury removal in the presence of SO<sub>2</sub>; however, SO<sub>2</sub> suppressed mercury removal irrespective of the presence of O<sub>2</sub>. The promotion of mercury removal by the presence of O<sub>2</sub> may result from the Deacon reaction. However, SO<sub>2</sub> seemed to inhibit the Deacon reaction. It is thought that mercury species formed on AC through the Deacon reaction was HgCl<sub>x</sub> (including HgCl<sub>2</sub>), which decomposed and desorbed at around 300 °C. The high-temperature TPDD peaks were observed at around 500 °C in TPDD spectra of the spent sorbents used in mercury removal in the presence of Cl<sub>2</sub> (or high concentrations of HCl), SO<sub>2</sub>, O<sub>2</sub>, CO<sub>2</sub>, and H<sub>2</sub>O. This TPDD peak temperature range is very close to the decomposition temperature of HgSO<sub>4</sub>. We suggest that the high-temperature mercury desorption peaks are related to the decomposition of mercury species similar to mercury sulfate containing chlorine (HgS<sub>x</sub>O<sub>y</sub>Cl<sub>z</sub>) on AC.

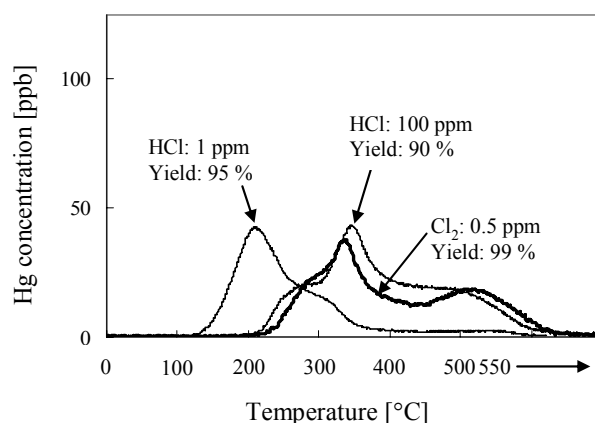


Fig.. Effects of the presence of 0.5 ppmv Cl<sub>2</sub> and 1, 100 ppmv HCl during mercury removal in the presence of 500 ppmv SO<sub>2</sub>, 5 % O<sub>2</sub>, 10 % CO<sub>2</sub> and 16 % H<sub>2</sub>O (SV = 2.4 × 10<sup>5</sup> h<sup>-1</sup>) on TPDD spectra.

## ■ Key word ■

Mercury removal, Activated carbon, TPDD

## ■ Affiliation ■

- 1) Master candidate, Graduate School of Environmental Science
- 2) Associate Professor, Dept. of Environmental Chemistry and Materials
- 3) Master candidate, Graduate School of Environmental Science
- 4) Professor Emeritus, Dept. of Environmental Chemistry and Materials
- 5) Associate Professor of Faculty of Environmental Science and Technology, School of Mechanical Engineering, Hangzhou Dianzi University, China

## ■ Printing ■

Energy & Fuels, 24 (8), pp 4241–4249, 2010.

Refereeing: Full paper, Language: English



## PEG-PLA nanoparticles prepared by emulsion solvent diffusion using oil-soluble and water-soluble PEG-PLA

MURANAKA Makoto<sup>1)</sup>, HIROTA Ken<sup>1)</sup> and ONO Tsutomu<sup>\*2)</sup>

### ■ Summary ■

Poly(ethylene glycol)-block-poly lactide (PEG-PLA) nanoparticles were prepared through the oil-in-water (O/W, ethyl acetate/water) emulsion technique using oil-soluble PEG-PLA in the presence of water-soluble PEG-PLA as a surfactant. The particle diameter decreased with increasing water-soluble PEG-PLA concentration, the smallest averaged diameter was 75 nm. From these results, it was found that water-soluble PEG-PLA acted as a surfactant which prevents further coalescence of droplets. In addition, the particles diameter decreased with increasing hydrophile-lipophile balance of oil-soluble PEG-PLA in the absence of water-soluble PEG-PLA. In contrast, the particle diameter was constant in the presence of water-soluble PEG-PLA. Therefore, the capability of water-soluble PEG-PLA as a surfactant was more excellent than that of oil-soluble PEG-PLA.

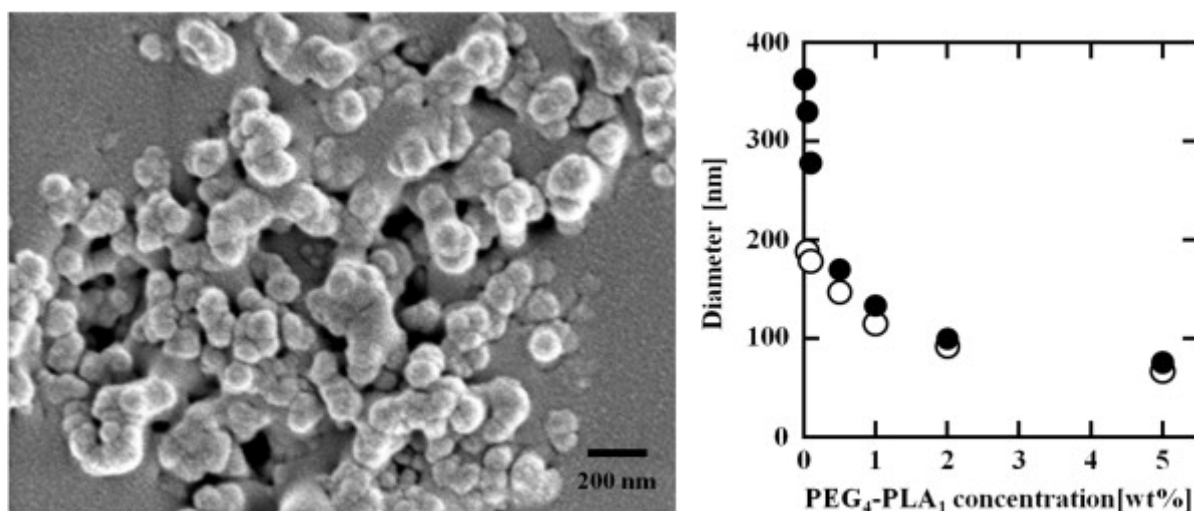


**Figure 1** (*left*) SEM image of PEG<sub>4</sub>-PLA<sub>29</sub> nanoparticles prepared by the emulsion solvent diffusion method using PEG<sub>4</sub>-PLA<sub>1</sub> as a surfactant; [PEG<sub>4</sub>-PLA<sub>29</sub>] = 3.3 wt.%, [PEG<sub>4</sub>-PLA<sub>1</sub>] = 5.0 wt.%. (*right*) The effect of PEG<sub>4</sub>-PLA<sub>1</sub> concentration on the diameter of PEG-PLA nanoparticles; open key: PEG<sub>4</sub>-PLA<sub>7</sub> (3.3 wt.%), closed key: PEG<sub>4</sub>-PLA<sub>29</sub> (3.3 wt.%).

### ■ Key word ■

Polylactide, Nanoparticle, Surfactant, Solvent diffusion, Nanoemulsion

### ■ Affiliation ■

1) Master candidate, Graduate School of Environmental Science

2) Associate Professor, Dept. of Environmental Chemistry and Materials

### ■ Printing ■

Materials Letters, 64, 969-971 (2010)

Peer-reviewed communication, Language: English

## Photocatalytic water treatment over $WO_3$ under visible light irradiation combined with ozonation

Shunsuke Nishimoto<sup>1)</sup>, Takayuki Mano<sup>2)</sup>, Yoshikazu Kameshima<sup>3)</sup>, Michihiro Miyake<sup>4)</sup>

### ■ Summary ■

Photocatalytic water treatment over bare  $WO_3$  under visible light irradiation combined with ozonation ( $O_3$ /vis/ $WO_3$ ) was investigated using an aqueous phenol solution as model wastewater. The  $O_3$ /vis/ $WO_3$  treatment exhibited a much higher total organic carbon removal than ozonation alone. Bare  $WO_3$  was found to function as an active visible-light-responsive photocatalyst for decomposition of organic compounds in the presence of ozone, which readily reacts with photoexcited electrons in the conduction band of  $WO_3$ .

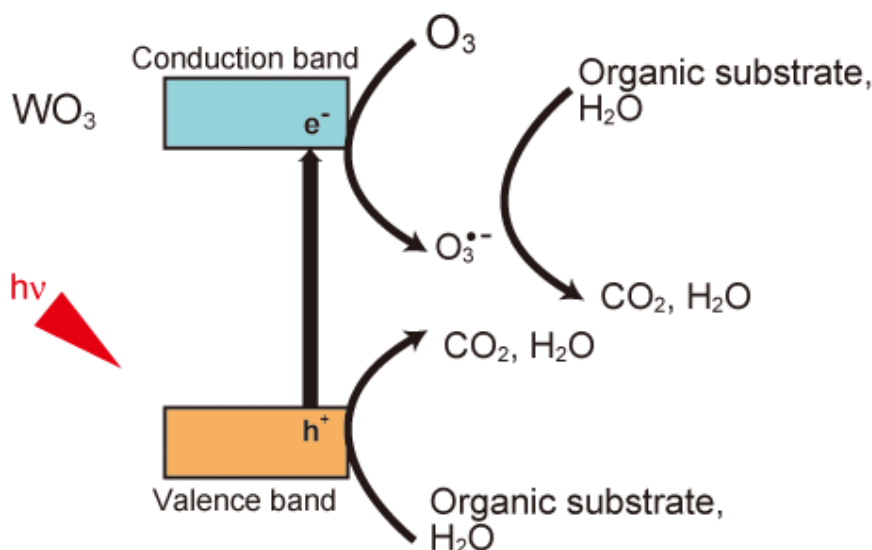


**Figure.** Schematic illustration of wastewater treatment using a  $WO_3$  photocatalyst combined with ozonation under visible light irradiation.

### ■ Key word ■

Visible-light-responsive photocatalyst, Tungsten oxide, Ozone, Phenol

### ■ Affiliation ■

- 1) Assistant Professor, Dept. of Environmental Chemistry and Materials
- 2) Master candidate, Graduate School of Environmental Science
- 3) Associate Professor, Environmental Management Center
- 4) Professor, Dept. of Environmental Chemistry and Materials

### ■ Printing ■

*Chem. Phys. Lett.*, **500**, 86-89 (2010).

## Steam reforming of naphthalene as model biomass tar over iron–aluminum and Iron-zirconium oxide catalysts

NOICHI Hiroyuki <sup>1)</sup>, UDDIN Md. Azhar<sup>2)</sup>, SASAOKA Eiji <sup>3)</sup>

### ■ Summary ■

The catalytic properties of iron-based mixed metal oxides such as iron–alumina (Fe–Al) and iron–zirconia (Fe–Zr) were investigated at 850 °C in a fixed bed reactor for the steam reforming of naphthalene as a model biomass tar compound. The effects of addition of copper species (CuO) to the iron based mixed metal oxide catalysts were also examined. For Fe–Al catalysts, the catalytic activities for naphthalene conversion increased with increasing Fe content except for 100Fe–0Al. The catalytic activities of Fe–Al and Fe–Zr were comparable at steady state conditions. Compound oxides were formed in the cases of Fe–Al, but not in Fe–Zr. A strong peak in the vicinity of  $2\theta = 45^\circ$  for metallic iron was observed after catalytic experiments in the XRD patterns of all catalysts, which could be related to the active sites of the catalysts. The addition of CuO increased the activities and stability of the Fe–Al catalysts. The reasons for catalytic activity enhancement due to CuO addition can be explained as follows: copper dispersed evenly in the compound oxides facilitate the reduction of iron oxides to metallic iron and prevent the catalytic deactivation due to decrease in surface area of the catalysts during the reaction.

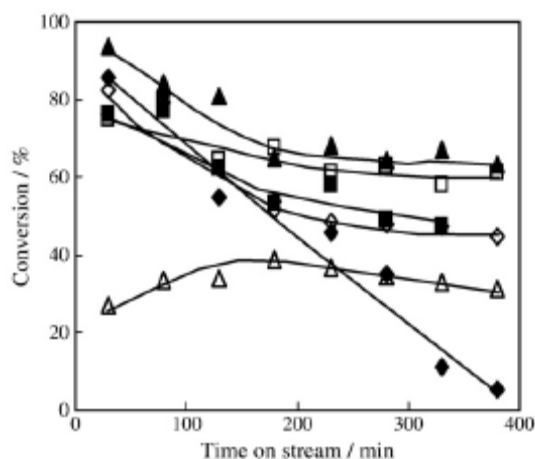


Fig. The catalytic activity of Fe–Al catalysts with different Fe content for the steam reforming of naphthalene at 50 °C (○ 30Fe–70Al, 40Fe–60Al, ■ 50Fe–50Al, □ 60Fe–40Al, ▲ 70Fe–30Al, △ 100Fe).

### ■ Key word ■

Biomass, Tar decomposition, Naphthalene, Iron oxide catalysts

### ■ Affiliation ■

- 1) Master candidate, Graduate School of Environmental Science
- 2) Associate Professor, Dept. of Environmental Chemistry and Materials
- 3) Professor Emeritus, Dept. of Environmental Chemistry and Materials

### ■ Printing ■

Fuel Processing Technology, 91, pp.1609–1616, 2010.

Refereeing: Full paper, Language: English

## Phase separation of borosilicate glass containing sulfur

SAIKI Keiji<sup>1)</sup>, SAKIDA Shinichi<sup>2)</sup>, BENINO Yasuhiko<sup>3)</sup>, NANBA Tokuro<sup>4)</sup>

### Summary

A  $10\text{Na}_2\text{S} \cdot 30\text{B}_2\text{O}_3 \cdot 60\text{SiO}_2$  (mol%) glass was prepared, and the changes in glass structure and chemical state of sulfur caused by phase separation were investigated. In the as-prepared and heat-treated glasses, sulfur was present as  $\text{S}^{2-}$  anion and polysulfide  $\text{S}_2^{2-}$  and  $\text{S}_3^{2-}$  anions, and Si-S and B-S bonds were not confirmed. A phase separation by spinodal decomposition was observed after heat-treatment, where sulfur was preferentially distributed to borate-rich phase. Even after the phase separation, formation of non-bridging oxygen was not recognized. The preferential distribution of sulfur anions in the present glass was explainable on the basis of the change in population of sodium ions, which compensated the negatively-charged sulfur anions.

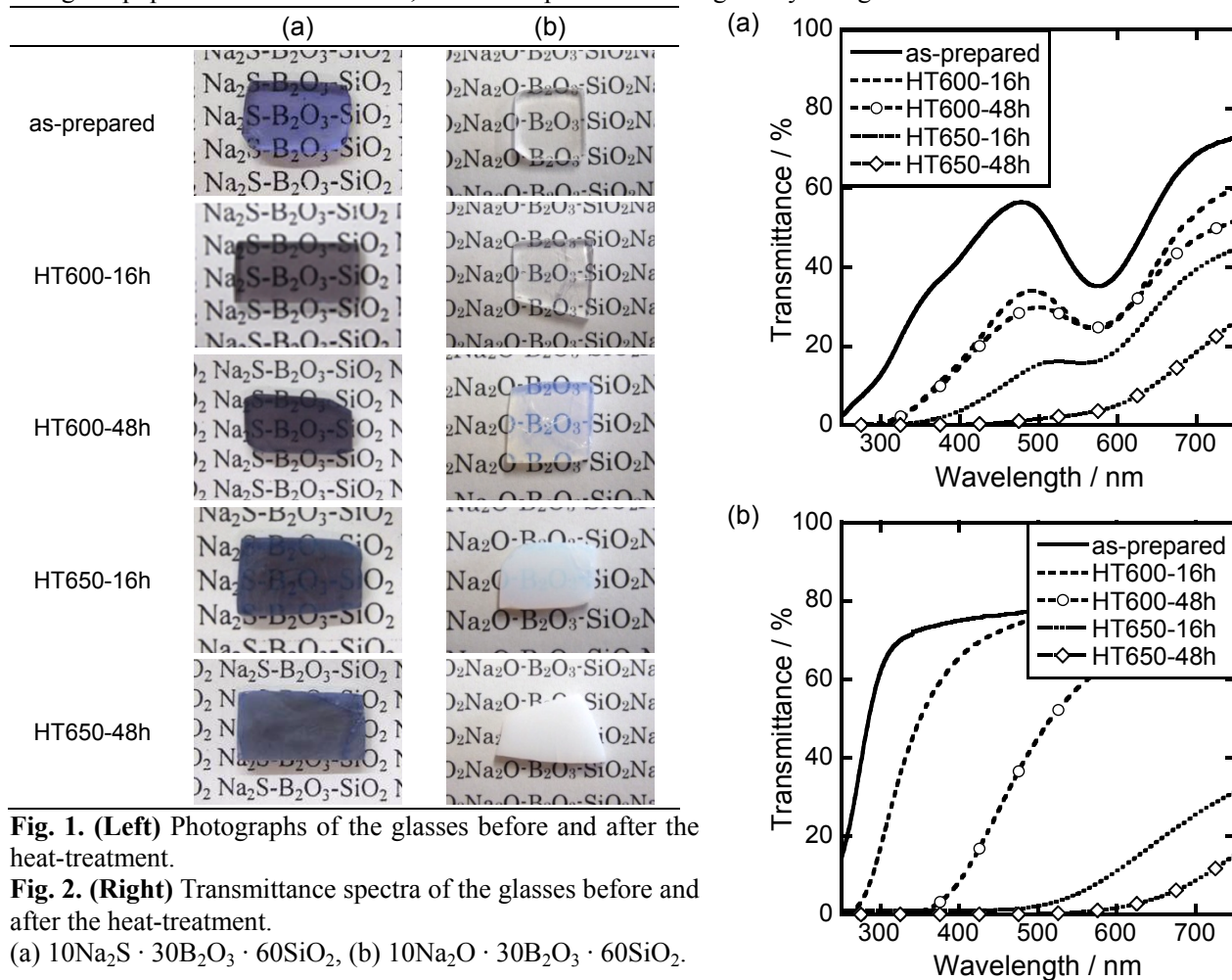


**Fig. 1. (Left)** Photographs of the glasses before and after the heat-treatment.

**Fig. 2. (Right)** Transmittance spectra of the glasses before and after the heat-treatment.

(a)  $10\text{Na}_2\text{S} \cdot 30\text{B}_2\text{O}_3 \cdot 60\text{SiO}_2$ , (b)  $10\text{Na}_2\text{O} \cdot 30\text{B}_2\text{O}_3 \cdot 60\text{SiO}_2$ .

### Key word

Phase separation, Borosilicate glass, Chemical state of sulfur, Glass structure

### Affiliation

- 1) Master candidate, Graduate School of Environmental Science
- 2) Assistant Professor, Environmental Management Center
- 3) Associate Professor, Dept. of Environmental Chemistry and Materials
- 4) Professor, Dept. of Environmental Chemistry and Materials

### Printing

Journal of the Ceramic Society of Japan, Vol. 118(7), pp. 603-607, 2010.7.

Peer-reviewed full paper, Language: English

## Electrode properties of the Ruddlesden-Popper series, $\text{La}_{n+1}\text{Ni}_n\text{O}_{3n+1}$ ( $n = 1, 2$ and $3$ ), as intermediate-temperature solid oxide fuel cells

Suguru Takahashi<sup>1)</sup>, Shunsuke Nishimoto<sup>2)</sup>, Motohide Matsuda<sup>3)</sup>, Michihiro Miyake<sup>4)</sup>

### ■ Summary ■

The Ruddlesden–Popper phases,  $\text{La}_{n+1}\text{Ni}_n\text{O}_{3n+1}$  ( $n=1, 2$ , and  $3$ ), were synthesized by a solid-state reaction for use as cathodes in an intermediate-temperature ( $500^\circ\text{--}700^\circ\text{C}$ ) solid oxide fuel cell. The samples crystallized into an orthorhombic layered perovskite structure. The overall electrical conductivity increased with the increase of  $n$  in the intermediate temperature range. Single test-cells, which consisted of samarium-oxide-doped ceria (SDC;  $\text{Sm}_{0.2}\text{Ce}_{0.8}\text{O}_x$ ) as an electrolyte, Ni–SDC cermet (Ni–SDC) as an anode, and  $\text{La}_{n+1}\text{Ni}_n\text{O}_{3n+1}$  as a cathode, were fabricated for measurements of cell performance at  $500^\circ\text{--}700^\circ\text{C}$ . Current interruption measurements revealed that both the ohmic and overpotential losses at  $700^\circ\text{C}$  decreased with the increase of  $n$ .  $\text{La}_4\text{Ni}_3\text{O}_{10}$  was found to exhibit the best cathode characteristics in the  $\text{La}_{n+1}\text{Ni}_n\text{O}_{3n+1}$  series. Maximum test-cell power densities with  $\text{La}_4\text{Ni}_3\text{O}_{10}$  ( $n=3$ ) were 10.2, 36.5, and  $88.2\text{ mW/cm}^2$  at  $500^\circ$ ,  $600^\circ$ , and  $700^\circ\text{C}$ , respectively.

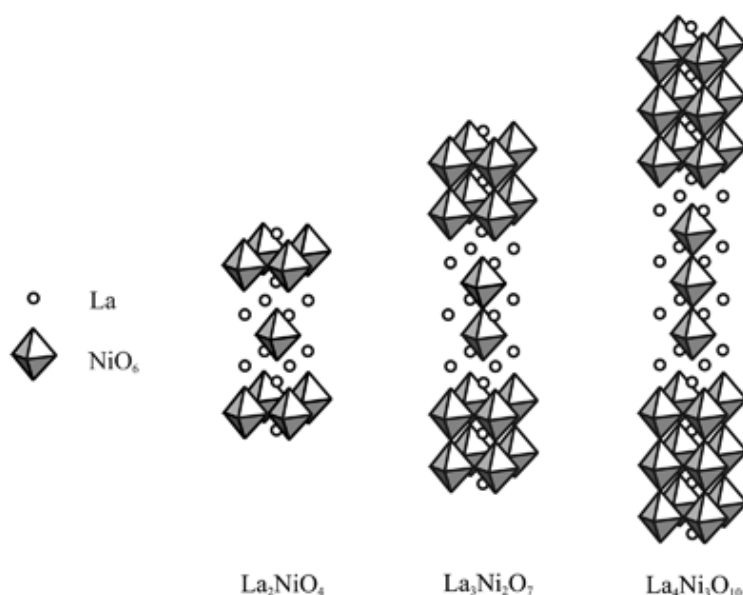


**Figure.** Structural illustration of the Ruddlesden–Popper phases,  $\text{La}_{n+1}\text{Ni}_n\text{O}_{3n+1}$  ( $n=1, 2$ , and  $3$ ).

### ■ Key word ■

SOFC, Layered perovskite, Cathode material

### ■ Affiliation ■

- 1) Master candidate, Graduate School of Environmental Science
- 2) Assistant Professor, Dept. of Environmental Chemistry and Materials
- 3) Professor, Kumamoto University
- 4) Professor, Dept. of Environmental Chemistry and Materials

### ■ Printing ■

*J. Am. Ceram. Soc.*, **93**, 2329-2333 (2010)

Peer-reviewed full paper, Language: English

## A versatile biodegradable polymer with a thermo-reversible/irreversible transition

TANIMOTO Fumiaki<sup>1)</sup>, KITAMURA Yoshiro<sup>3)</sup>, ONO Tsutomu<sup>\*2)</sup> and YOSHIZAWA Hidekazu<sup>3)</sup>

### ■ Summary ■

A versatile biodegradable thermoresponsive polymer was developed. The polymer has succinimide and isopropylasparamide segments and exhibits a phase transition with thermoreversibility that can be controlled by changing the polymer composition. With fewer succinimide units, the polymer exhibits the type of thermo-reversible phase transition that is characteristic of poly(N-isopropylacrylamide) (PNIPAAm). The polymer with a higher proportion of succinimide units exhibits a thermo-irreversible phase transition, resulting in the formation of nanospheres that are stable below the transition temperature. The stable nanospheres are generated by dehydration and subsequent conformational stabilization through an interaction between imide rings. This thermoirreversible phase transition in water provides a simple, oil-free preparation of biodegradable nanospheres.

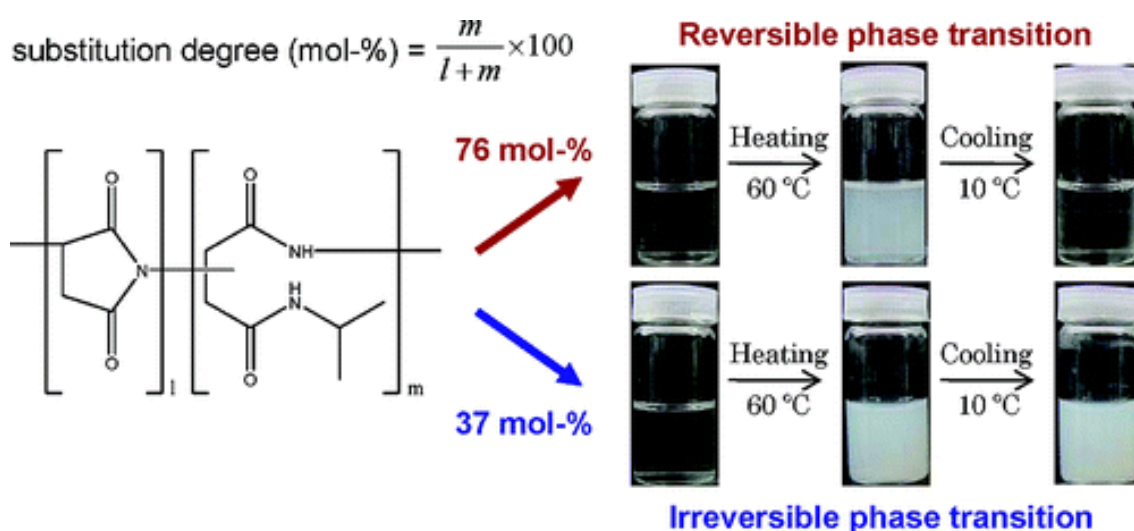


**Figure 1** Thermoresponsiveness of aqueous solutions of IPA-PSI with various degrees of substitution (DS). Change in appearance of aqueous IPA-PSI with DS = 76 (upper) and DS = 37 mol % (lower).

### ■ Key word ■

Thermoresponsive polymer, Irreversible phase transition, Poly(aspartic acid), Poly(succinimide)

### ■ Affiliation ■

- 1) Master candidate, Graduate School of Environmental Science
- 2) Associate Professor, Dept. of Environmental Chemistry and Materials
- 3) Professor, Dept. of Environmental Chemistry and Materials

### ■ Printing ■

ACS Applied Materials & Interfaces, 2, 606-610 (2010)

Peer-reviewed Full-paper, Language: English